Mechanistic Agent-based Damage and Repair Models as Hypotheses for Patterns of Necrosis Caused by Drug Induced Liver Injury

Andrew K Smith[1], Glen E.P. Ropella[2], Neil Kaplowitz[3], Murad Ookhtens[3], and C. Anthony Hunt[1]

[1]**Bioengineering and Therapeutic Sciences, University of California, San Francisco, CA 94143;** [2]**Tempus Dictum, Inc. Milwaukie, OR 97222;** [3]**Division of Gastrointestinal and Liver Diseases, Division of Gastrointestinal and Liver Diseases, Department of Medicine, Keck School of Medicine, University of Southern California, Los Angeles, CA 90033**

drandrewksmith@gmail.com   gepr@tempusdictum.com   a.hunt@ucsf.com
kaplowit@usc.edu   murad@usc.edu

Keywords: mechanisms, multiscale, methodology, In Silico Liver, necrosis

Abstract

Increasing model reuse and facilitating repurposing is expected to expand simulation use for better explaining biological phenomena. We demonstrate doing so in the context of liver diseases caused by toxic exposure to xenobiotics. A clinical goal is improved mechanistic explanations of how damage is generated, which can lead to new strategies to block and/or reverse injury. A goal for this work is to provide concrete, plausible explanations for acetaminophen induced liver injury (AILI) in mice. We instantiate mechanistic hypotheses that map to cellular damage and repair pathways and begin identifying plausible simulated causal cascades capable of generating the characteristic AILI spatial and temporal patterns. We use discrete event simulation of agent-based, multiscale, biomimetic models and Monte Carlo sampling. We use an Iterative Refinement protocol for implementing and validating/falsifying mechanistic hypotheses on a previously validate In Silico Liver. We simulated an observed necrosis pattern. Further approach improvement will yield new methods that combine iterations of in-silico and wet-lab experiments.

Abbreviations: APAP: acetaminophen; AILI: APAP induced liver injury; CV: central vein; D: damage objects; DILI: drug induced livery injury; GSH: glutathione and analog counterpart objects; ISL: In Silico Liver; IR: Iterative Refinement; NAPQI: reactive metabolite of APAP; N: analog counterpart objects of NAPQI; PV: portal vein; R: Repair objects; SM: similarity measure; SCyc: simulation cycle; TA: targeted attribute

1. INTRODUCTION

Currently, most biomedical models exist in isolation. Consequently, contributions from simulations to the advance of biomedical science remain limited, even though it is recognized that advances in biomedical science require more explanatory mechanistic models. From a simulation engineering perspective, one of our goals is to increase model and component reuse and facilitate repurposing. So doing will lower barriers to expanded use of simulation in the pursuit of mechanistic models that better explain biological phenomena. This work demonstrates model reuse and repurposing and has provided lessons for improving both.

Drug induced livery injury (DILI) is the most common cause of acute liver failure, with acetaminophen (APAP) responsible for the majority [1]. Also, DILI is a major challenge for the pharmaceutical industry and regulatory bodies [2]. AILI exhibits several heterogeneous, multiscale features that are common to other liver diseases. The liver is susceptible to drug induced injury because of its central role in xenobiotic metabolism.

Liver anatomy and physiology complexity presents modeling and simulation challenge. The liver consists of many nearly polyhedral functional units called lobules. Lobules consist of interconnected vascular tubes (sinusoids), through which blood flows from the exterior portal vein (PV) to the central vein (CV). Hepatocytes contain enzymes that bind and metabolize xenobiotics. The space between the PV and CV is characterized as being divided into three zones, termed zonation, that vary in micro-anatomy and physiology. Hepatocytes located near the PV (Zone 1) have higher oxygen and nutrient concentrations than those located near the CV (Zone 3). Most importantly for AILI, Zone 3 hepatocytes are the primary sites of conversion of APAP to the reactive

metabolite called NAPQI. Following a toxic dose of APAP, necrosis (cell death) occurs initially and is more extensive in Zone 3. Spreading outward toward the PV follows [3].

Within hepatocytes, NAPQI initiates damage to cellular pathways, which in turn activates repair pathways. Pathways are networks of interacting cellular components, including macromolecular complexes and organelles, such as mitochondria. NAPQI reacts preferentially with glutathione, but also with mitochondrial proteins forming adducts [4][5]. Glutathione depletion indirectly increases naturally occurring yet damaging reactive oxygen/nitrogen species. Resulting adducts can cause mitochondrial dysfunction, including lowered cellular energy and increased reactive oxygen/nitrogen species [2]. The latter can react with proteins, lipids, or nucleic acids in DNA. Damaged proteins can be disaggregated and refolded or degraded [6]. Damaged DNA has its own set of specialized repair mechanisms [6]. Also, changes in redox homeostasis can lead to activation of transcription factors that control the expression of antioxidant enzymes and cofactors [2]. Continuing oxidative stress from reactive oxygen/nitrogen species leads to mitochondria dysfunction triggering activation/inhibition of signal transduction pathways. An important result is increased mitochondrial membrane permeability, which is a precursor to necrosis. Cell survival or death is determined in part by the balance of activated pro-death and pro-survival processes. The pace and consequences of these unfolding events depend on the magnitude and time course of NAPQI exposure along with the influence of zonation of the above processes.

In general, two basic methods are available for modeling and simulating damage and repair pathways to explain the patterns of necrosis over space and time. One approach is the application of systems of coupled ordinary differential equations compartmentalized into interacting components and evolved through time. Within well-defined systems under specific assumptions, that method is scientifically productive [7]. However, given the highly heterogeneous, variable, and uncertain nature of AILI, our In Silico Liver (ISL) platform required the flexibility and extensibility provided by combining agent-based modeling, discrete event simulation, and Monte Carlo sampling methods [8]. We need the flexibility and extensibility to explore and challenge a variety of similarly plausible mechanistic hypotheses of damage and repair.

2. APPROACH

Our five-stage approach combines the scientific method and good software engineering practices. First, a referent "targeted attribute" (TA) is selected from a list of TAs that we eventually wish to explain. A TA can be either qualitative, such as a description, or quantitative, such as data collected from wet-lab experiments. Second, a hypothesis is formulated as an in silico mechanism. The mechanism is a plausible causal cascade of events that is intended to produce a phenomenon analogous to the TA. The phenomenon is the product of temporal component interactions. Third, we refactor and add to extant mechanism code (from already studied analogs) to create the specified mechanisms. A series of simulation experiments are performed. Measurements, such as component numbers, event location, and timing, are measured and recorded. Fourth, simulation and referent results are compared using a "similarity measure" (SM). If the SM criterion is achieved, the analog has achieved a degree of validation. Finally, the validated analog's mechanism granularity is either increased parsimoniously or additional TAs are specified, and the process is repeated with the objective of falsifying (or not) the implemented mechanism. When the analog mechanisms with their embedded knowledge survive the challenge, the analog can stand as a plausible, concrete explanation of the targeted phenomena. For the above approach, mechanism (explanation) falsification is just as important as validation.

2.1 Agent-based Models

Salient characteristics of referent wet-lab experiments include pervasive uncertainty, sparse system information, and considerable variability [8]. They make distinguishing causes from effects difficult. Agent-based methods provide the flexibility, extensibility, and generality needed to assemble software mechanisms that are increasingly biomimetic during execution. We call variants of our agent-based models analogs in order to emphasize that simulated mechanisms are intended to be analogous to a particular biological counterpart. The liver is compartmentalized; for instance, proteins are contained in organelles, which are contained in cells, which are contained in tissue, etc. Analogs are similarly compartmentalized. Many biological processes are analogized as logical statements; for instance, if protein A binds to protein B; then protein B is activated. Our agents implement similar rule-base behavior when mediating interacting components. We require our analogs to be multiscale to mimic biological phenomena believed to involve components interacting at different functional levels. The variety of analog-to-wet-lab mappings (i.e. the comparison of analog to referent attributes) is a direct measure of an analog's multiscaleness. A mapping has a spatial and temporal scale. Biological spatial scales typically correspond to functional "levels" being observed. Important biological scales are molecular, intracellular

(organelle), cell, tissue functional unit, organ, and organism. Executions of analogs can be measured at all but the organism scale. A wet-lab experiment's temporal scales typically correspond to sets of measurements at intervals. Likewise, the state of different analog components (often at different spatial scales) updates at different time steps/simulation cycles. Our goal is that analog measurements made at different spatial and temporal scales during the same simulation can be mapped separately and quantitatively to wet-lab measurements also spanning different spatial and time scales. Achieving that goal requires relational grounding throughout the analog [9]. Consequently, specific mapping models are expected to vary.

2.2 From Qualitative to Quantitative Validation

We need discrete event simulations to facilitate staged transition from qualitative. Qualitative validation must precede quantitative validation. Our qualitative validation targets are primarily patterns of relative sequences of events. Requiring particular sequence timings makes those validation targets temporally quantitative. The latter can be achieved using relatively coarse grain, parsimonious analogs. Wet-lab measurements made at different temporal and spatial granularities are always proportional. However, mappings from coarse and finer grain analog phenomena to wet-lab counterparts need not be proportional.

2.3 Monte Carlo Sampling

Currently, even with a plethora of knowledge, complex biological systems have many sources of variability and uncertainty that must be accounted for in some way in our simulations. We use Monte Carlo sampling to introduce both. For example, wet-lab experiments exhibit variabilities across samples. Analogously, we vary the spatial architecture of our analogs pseudo-randomly, repeat simulations and average results. Metabolism and other biochemical reactions are inherently probabilistic. We mimic associated uncertainties using probabilistic parameters that specify a probability of interaction or reaction within a simulation cycle. In addition, some probabilistic parameters are not scalar but vary over space. During analog execution, agent-mediated Monte Carlo sampling of probability distributions over space and time determine the location and timing of injury and repair phenomena.

3. METHODS

The referent is the mouse liver lobule. The TA is the observation of necrosis starting near the CV following a toxic dose. The SM is qualitative: simply observe

considerably more Death events near the CV than PV. We began with the use case of a previously validated ISL. During experiments, we adhered to the Iterative Refinement Protocol (IR protocol) and observed and measured relevant patterns, focusing on Metabolite numbers, Death event location, and timing thereof.

3.1 Use Case

Our use cases are in silico experiments that mimic the wet-lab experiments from which the TAs were selected.

3.2 The IR Protocol

Our core method is the IR protocol. We approach credible validation by cycling many times through the IR Protocol. A validation target is achieved when a SM is attained for a TA. We have applied the IR protocol successfully [10]. The relationships between validation targets, parsimonious mechanistic granularity, and explanatory power through validation/falsification embodied in the IR protocol is illustrated in Figure 1.

1) Gather possible TAs from the literature and other sources, taking into account the mechanistic granularity that may be required to validate and select one. The choice is constrained by a strong parsimony guideline and requirement that we do not disrupt already achieved TAs.

2) Increase mechanistic granularity parsimoniously. Mechanistic over-granularization can greatly expand analog behavior space and the set of parameterizations that enable validation. A good practice is to take smaller steps that mostly fail (Step 8), because in doing so we accumulate evidence for how and why we are shrinking mechanism space (Figure 1). In this work, the implemented damage and repair mechanisms increase mechanistic granularity by adding damage and repair objects. Coarse grain analog objects, such as current damage objects in this work, have no direct inter-hepatocyte counterpart. Rather, they are hypothesized to map to a set of similarly influential molecular markers.

3) Update SMs, their target values, and how they are used. The qualitative SM was modified slightly so that necrosis means location and timing of Death events.

4) Specify a mechanism revision hypothesis. Typically, there are multiple, equally possible or plausible options. In this work, the damage mechanism was revised to include pro-death damage objects.

5) Specify an analog revision plan. So doing may include (or not) revising modules, components, model use case(s), parameters, rules, and parameterization ranges. We modified parameterizations.

6) Conduct and measure many simulation experiments. Random sampling of a relatively small region of parameter space enables us to observe a consistent analog phenotype.

7) A failed mechanism, even when coarse grain, provides new knowledge and shrinks plausible mechanism space. If it fails, then return to Step 4 or 5. If successful, then we have achieved a degree of validation. In this work, we cycled through Steps 4-6 several dozen times before achieving the validation target.

Afterward, we have two options: a) increase stringency of one or more SMs; so doing may falsify the mechanism. For example, require a certain percent of necrosis (Death events) within a certain distance from the CV. Or b) select another TA from the list. It is not unusual for insights achieved or observations made during an IR Protocol cycle to alter opinions about and priorities of listed TAs. A classic approach is to make a prediction that motivates or supports subsequent wet-lab experimentation, and the preferred outcome is that the results will validate the in silico hypothesis. That is not the case here.

3.3 Validated In-Silico Liver

We start with a previous in-silico liver (ISL) that has achieved drug clearance [11] and enzyme induction/elimination validation targets [12]. The ISL is described in detail in [12]. Briefly a liver lobule is represented by a directed graph of sinusoid segments (SSs), vascular tubes, flowing from the PV to the CV. There are three zones from PV to CV. The periportal Zone 1 has the most SS nodes (45) and significant intrazone edges (20). Zone 2 has fewer nodes (20) and fewer intrazone edges (10). The perivenous Zone 3 has three nodes and 0 intrazone edges. APAP objects are injected into the PV, flow through the SS network and those that exit the ISL are collected and counted at the CV. Each SS consists of a concentric layering of three cylindrical grids wrapped around a core queue. The core conducts a laminar flow of perfusate (maps to blood) along the length of the SS. The innermost Grid A models more turbulent and viscous flow along the endothelial lining of the sinusoid by using a pseudo-random movement biased toward the SS outlet. Grid B is partially populated by Endothelial Cell objects into which Solute (but not Marker) objects can partition, and which partially blocks lateral Marker movement. Solute that makes it past the Endothelial layer enters Grid C, which models the Space of Disse and is partially populated by Hepatocyte objects. Both Cell types contain Binder objects that can sequester compound for some number of simulation cycles (SCycs). Currently 1 SCyc

maps to 1 second. Hepatocytes contain Binders called Enzymes, which may metabolize bound compound according to a probabilistic parameter. What concerns us in this work is intra-hepatocyte mechanisms, specifically what happens after NAPQI formation.
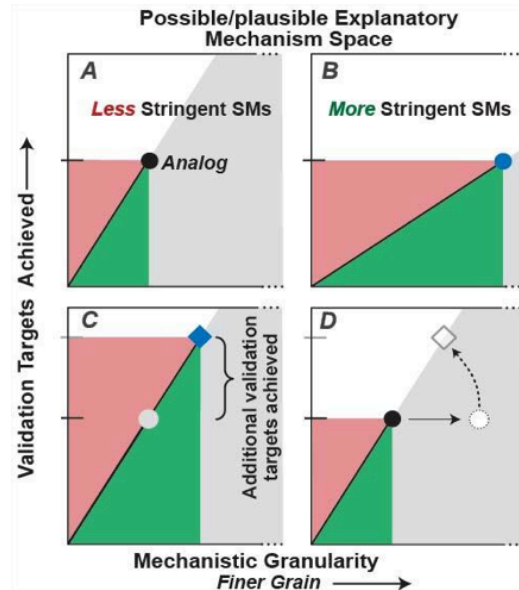
Figure 1 Illustrations of relationships between validation targets, parsimonious mechanistic granularity, and explanatory power embodied in the IR protocol. The green-gray transition represents the divide between validated, parsimonious mechanisms and hypothetical, possible mechanisms: Occam's barrier. The analog mechanism just inside the red area is concretely false, whereas the finer grain analog mechanism just inside the green area is concretely explanatory. ***A***: An illustration of a previously validated analog, such as the ISL. The y-axis hash marks indicate currently achieved validation targets. ***B*** & ***C***: We can enhance explanatory power and shrink the space of equally plausible mechanisms by increasing the stringency for one or more SMs (***B***) or incrementally increasing validation targets (***C***). Either ***B*** or ***C*** activity can falsify the analog in ***A***. ***D***: An illustration of increasing mechanistic granularity without either changing SM stringency or incrementally increasing validation targets. The resulting, finer grain mechanism represented, by the diamond, is only a hypothesis (a mechanistic prediction) because it has achieved no *new* validation targets.

3.4 Damage and Repair Mechanisms

Various AILI hypotheses focus on aspects of cellular injury from different granularity perspectives. We employ our simulation methods to combine multiple perspectives while refining and combining hypotheses. The following

general theory of AILI is widely accepted: NAPQI first reacts with and depletes glutathione (GSH). GSH synthesis can be viewed as a repair mechanism. Once GSH is depleted, reactive oxygen/nitrogen species accumulate damaging macromolecules and organelles, and that leads to oxidative stress within and outside mitochondria. A dynamic damage–repair struggle ensues, signaling different pathways simultaneously. When damage overwhelms repair mechanisms, stress signals trigger necrosis. A complication is a hepatocyte's PV-to-CV location.

In ISL analogs, parameters controlling most events are probabilities of event occurrence per SCyc, and are designated p(·) and summarized at the top of Figure 2. Location-dependent values of the three key APAP metabolism parameters are plotted in the upper left of Figure 2. Enzyme objects within Hepatocytes use those parameterization rules to specify the probability of metabolism/SCyc. At PV the probability of forming A (maps to glucuronidation), B (maps to sulfation), or N (maps to NAPQI) is the same. Less A and B but more N is generated towards the CV. Once formed, p(A, B removal from Cell) = 0.5. N cannot exit the Cell back into Blood but can enter the bile canal.

Prior to the work described in Figure 2, several mechanisms were implemented and challenged following the IR Protocol. The validation target was that damage near the CV (in Zone 3) be at least 10-fold greater than elsewhere. We envisioned some level of that damage acting as a "tipping point." An example follows. Drawing on accepted conceptual mechanisms, we specified that N react in two ways: 1) it depletes Hepatocyte GSH. GSH and N combine stoichiometrically eliminating an N and depleting the Cell's GSH pool; and 2) it directly initiates other events (not specified) that form an analog damage object, D, and eliminate an N. We specified a lobular location dependent GSH depletion threshold (shown at top of Figure 2); GSH depletion is dependent upon a threshold value specified for all Cells. Prior to reaching the threshold, p(N removal) = 0.9. Each N removal reduces the threshold value by one. Once the threshold is reached, GSH is "depleted." Thereafter, $p(N \rightarrow D) = 0.5$ and is location-independent (i.e. constant along the PV-to-CV distance). GSH can be depleted and some D can form all within one SCyc. The reason why is the following: inter-Hepatocyte events update four times (steps) during a single Lobule SCyc. Some Cells contain several Enzyme objects, each of which can metabolize APAP and generate N during one step; during another step the N may deplete GSH or produce D. There is experimental evidence that normal GSH levels decrease PV-to-CV, so we made the GSH depletion threshold location-dependent. Nevertheless, ISL experiments utilizing the above GSH depletion and damage

creation mechanisms were falsified: they failed to achieve the validation target.

To expand the mechanism with the objective of achieving the validation target (IR Protocol Step 7), we introduced a location-dependent repair mechanism. An analog Repair event corresponds to removing a D and replacing it with an R object with probability $p(D \rightarrow R)$. Using a decreasing sigmoid function from PV-to-CV, we achieved the validation target (results not shown). However, literature reports document that some damage is repaired easily whereas repair of other damage can be problematic. A parsimonious solution is to "split" D into D1 and D2, where the latter are repaired separately with different location dependences. Specifically, we stipulated that after GSH depletion, $p(N \rightarrow D1, D2) = 0.5$, and $p(D1 \rightarrow R)$ and $p(D2 \rightarrow R)$ have different location dependences. Because pericentral pO_2 is chronically low, which increases the risk of oxidative damage, the literature consensus is that some repair functions are normally elevated in zone 3 relative to zones 1 and 2; therefore, $p(D1 \rightarrow R)$ maps to those repair processes. In addition, we conjectured that some mitochondrial damage might be less effectively repaired as pO_2 decreases; therefore, $p(D2 \rightarrow R)$ maps to those repair processes. The necrosis trigger mechanism was a simple threshold: if number (D2) > threshold value, then the cell will die. With those mechanisms implemented, we performed simulations using 24 Monte Carlo analog variants. Amounts of generated objects (i.e., A, B, N, D1, D2, R) along with location/timing of Death events were measured, and the results averaged.

4. RESULTS

The results in Figure 2 were obtained after testing several different parameterizations of both D1 and D2 repair mechanisms, and several necrosis triggers. In Figure 2, the D2 threshold per Cell = 12.5; If exceeded, the cell dies. Focusing on relative patterns, we ignored lag-times and specified that when triggered, Death event be scheduled for the next SCyc. Lowering the necrosis threshold and increasing APAP dose, absent saturable processes, achieves the same outcomes. Incrementally lowering the necrosis threshold results in more dead Cells closer to PV at all times. In this ISL analog, a dead hepatocyte simply stops metabolizing and does not "rupture," yet APAP does wash out. Additional Death events would have occurred had simulation duration been extended.

During the above experiment, APAP was infused for a constant rate for the initial 120 SCycs. For each Zone, N, D1, and D2 have similar temporal profiles (panels A-C). In Zone 1, those objects rapidly increase, plateau, and then, after 120 minutes, rapidly decrease. In Zone 2, they increase

5
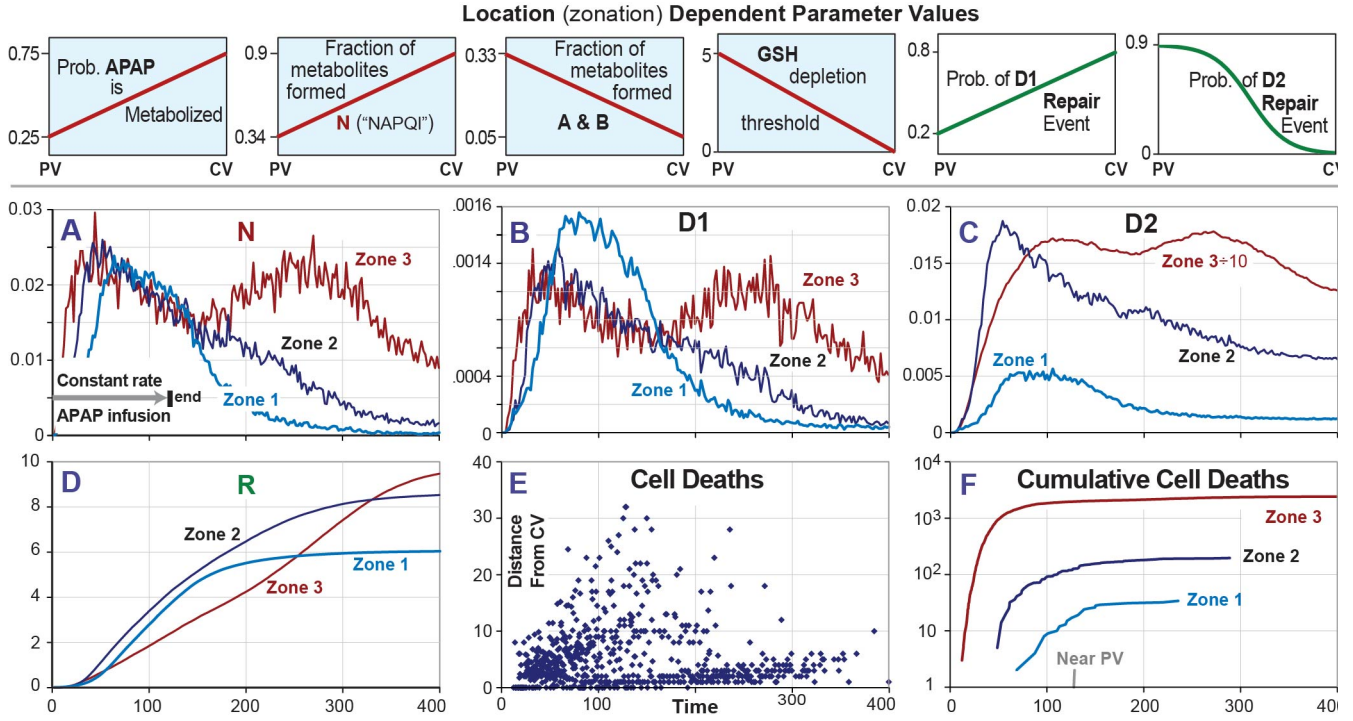
Figure 2 Top: Parameters responsible for AILI in the ISL analog used in this work. All graphs specify lobular location dependent parameterizations described in the text. The shaded boxes are from a previously validated ISL analog. 354K APAP objects were infused at a constant rate over 120 cycles. Mean APAP metabolizing enzymes/hepatocyte increase 4x PV-to-CV. Hepatocytes/lobule x 24 lobules = 336,000 for this experiment. 2,865 hepatocytes died within 400 cycles. In this ISL, a dead hepatocyte simply stops working. It does not fall apart (however, any APAP washes out). Additional deaths would have occurred had simulation duration been extended. **A–D**: Plots of mean values of N, D1, D2, and R, respectively, per hepatocyte vs simulation cycles (i.e. time). **E**. Death events at a specific time vs cell location as distance from CV. **F**. cumulative Death events per Zone 1, 2, 3, and near PV over time (y-axis is log scale). Zone 3 < 11 distance from CV, Zone 2 < 21, Zone 1 < 31, near PV > 31. Zone 3 contained 91% of Death events.

rapidly then gradually decrease after ~50 SCycs. In Zone 3, they exhibit a distinctive double maximum profile, with the second increase/decrease beginning after 120 SCyc. This second "hill" most likely results from depleted GSH so less N removal, and then an increase in N creation as APAP moves into Zone 3. Having D1 and D2 profiles mirror the N profiles is reasonable because D1 and D2 are created from N. Like the previously validated ISL, the D2 maximum in Zone 3 is ~10x the maximum in Zone 2, which is ~3x the maximum in Zone 1. Both D1 and D2 damage mechanisms create R. For all Zones, R profiles are increasing sigmoids, with Zone 3 showing evidence of a double sigmoid that may be a consequence of conflating repair parameterizations. Because R objects are neither "metabolized" nor removed, the cumulative profiles in Figure 2D approach asymptotes with Zone 1 < Zone 2 < Zone 3.

The ISL parameterizations at the top of Figure 2

achieved validation targets. The distance from the CV and time of death is plotted for Death events in Figure 2E. The panel shows Death events occurring first adjacent to the CV. Over the initial ~150 SCycs, Death events spread away from the CV toward the PV. Cumulative Death events for each Zone are plotted in Figure 2F. In Zone 3, early Death events increase rapidly, but after ~75 minutes Death rate slows for the duration of the simulation. Following a lag period, the pattern is similar in Zone 2. However, there were no Deaths after 289 SCyc. The Zone 1 pattern is also similar; there were no Deaths after 236 SCyc. There were only two Deaths near the PV.

5. DISCUSSION

We demonstrate ISL reuse and repurposing to improve explanatory mechanistic insight into emergence of damage patterns within hepatic lobules following exposure to a

toxic APAP dose. We implemented and achieved a degree of validation for a coarse grain analog damage and repair mechanism hypothesized to have liver lobule counterparts. The initial causal ISL event is conversion of an N object into either D1 or D2 objects. The next influential event is conversion of D2 into R.

How biomimetic are these mechanisms? Should damage and repair be thought of as components or processes? The following are examples of issues or limitations that will need to be addressed as we move forward.

Damage objects can be mapped roughly to objects in real hepatocytes, such as protein-adducts, reactive oxygen/nitrogen species, and dysfunctional mitochondria. In mice, those damage products can also cause further damage. An R object maps to reduction in any cellular damage that can influence necrosis. The conversion of N to D1/D2 and D1/D2 to R are single analog events yet we envision that they map to inter-hepatocyte processes involving sequences of events. As a consequence of the mechanism's current coarse grain and the parsimony guideline, we do not yet have specific analog objects that map to mitochondria, even though domain experts believe that mitochondria play central roles in both processes. They can be included in ISLs easily when the IR Protocol cycle requires doing so.

The Figure 2 damage and repair mechanism maps to a conflation of many pathways believed important within hepatocytes. They may also include several having extracellular sources. A goal is to make ISL components and interactions increasingly concrete, specific, and explicit. As we do so, we will replace conflated components and events with finer grain counterparts necessary to achieve an expanding set of prespecified validation targets. Several attributes, once included in the expanded set of TAs, are expected to force damage mechanisms to become finer grained. Examples include TAs related to reactive oxygen/nitrogen species [14] and endoplasmic reticulum stress [15] for damage. Expanding to include TAs related to mitochondrial fission, mitophagy, and other adaptive responses [16] are expected to force repair mechanisms to become finer grained. The process known as *mitochondrial permeability transition* is also important. It is caused by oxidative damage and precedes Death. We therefore anticipate mitochondria counterparts becoming integral to validation against an increasing variety of TAs having more stringent SMs. Other mechanistic hypotheses related to damage and repair may map to extra-hepatocyte sources. For example, damage mediated by connexins connecting adjoining hepatocytes [17], signals released from injured sinusoidal endothelial cells (SEC) [18], the repair response of the innate immune system (Kupffer cells and neutrophils) elicited from dying cells, and liver regeneration to prevent the spread of necrosis and/or replace dead hepatocytes [1]. Furthermore, dying cells release damage associated molecular patterns believed to trigger death in some neighboring cells. The process is a further extension of the feedback idea of damage causing more damage. Understanding damage amplification is expected to be crucial to a more detailed mechanistic explanation of toxicity-induced necrosis.

6. FUTURE DIRECTION

The results presented demonstrate ISL analog and component reuse and repurposing to improve explanatory mechanistic insight into AILI. These biomimetic analogs are continuously evolving. With every cycle through the IR Protocol the analog's mechanistic and component granularity can increase and its phenotype can expand. With further lowering of the barrier to model and component reuse and repositioning plus diminished need for refactoring, we envision explanatory mechanistic analogs becoming increasingly coupled to wet-lab experiments to shrink the space of plausible mechanistic explanations and improve actionable insight while guiding further research. We expect that achieving expanded sets of validation targets will force mechanisms to become increasingly fine grain and thus more credible. Having components that map to mitochondria is an example. Having easily reused and repurposable components also makes it easier to instantiate and challenge (both in silico and wet-lab) competing yet equally explanatory causal hypotheses. Differences in the unfolding of competing, simulated cascades can be challenged using focused wet-lab experiments. Results may falsify some and enable rank-ordering the survivors in terms of plausibility. We envision such in-silico/wet-lab cycles of hypothesis competition and refinement continuing well into the future.

REFERENCES

[1] Jaeschke, H.; C.D. Williams; A. Ramachandran; M.L. Bajt. 2012. "Acetaminophen hepatotoxicity and repair: the role of sterile inflammation and innate immunity." *Liver Int*. 32(1):8-20.

[2] Han, D.; L. Dara; S. Win; T.A. Than; L. Yuan; S.Q. Abbasi; Z.X. Liu; N. Kaplowitz. 2013. "Regulation of drug-induced liver injury by signal transduction pathways: critical role of mitochondria." *Trends Pharmacol Sci* 34(4):243-53.

[3] Jaeschke, H.; M.R. McGill; A. Ramachandran. 2012. "Oxidant stress, mitochondria, and cell death mechanisms in drug-induced liver injury: lessons learned from acetaminophen hepatotoxicity." *Drug Metab Rev* 44(1):88-106.

[4] Yang, X.; J. Greenhaw; A. Ali; Q. Shi; D.W. Roberts; J.A. Hinson; L. Muskhelishvili; R. Beger; L.M. Pence; Y. Ando; J. Sun; K. Davis; W.F. Salminen. 2012. "Changes in mouse liver protein glutathionylation after acetaminophen exposure." *J Pharmacol Exp Ther*. 340(2):360-8.

[5] Yang, X.; J. Greenhaw; Q. Shi; D.W. Roberts; J.A. Hinson; L. Muskhelishvili; K. Davis; W.F. Salminen. 2013. "Mouse liver protein sulfhydryl depletion after acetaminophen exposure." *J Pharmacol Exp Ther*. 344(1):286-94.

[6] Gu, X.; J.E. Manautou. 2012. "Molecular mechanisms underlying chemical liver injury." *Expert Rev Mol Med*. Feb 3;14:e4.

[7] Bhattacharya, S.; L.K. Shoda; Q. Zhang; C.G. Woods; B.A. Howell; S.Q. Siler; J.L. Woodhead; Y. Yang; P. McMullen; P.B. Watkins; M.E. Andersen. 2012. "Modeling drug- and chemical-induced hepatotoxicity with systems biology approaches." *Front Physiol* 3:462.

[8] Hunt, C.A.; R.C. Kennedy; S.H. Kim; G.E. Ropella. 2013. "Agent-based modeling: a systematic assessment of use cases and requirements for enhancing pharmaceutical research and development productivity." *WIREs Syst Biol Med*. 5(4):461-80.

[9] Hunt, C. A.; G.E. Ropella; T.N. Lam; A.D. Gewitz. 2011. Relational grounding facilitates development of scientifically useful multiscale models. *Theor. Biol. Med.*

[10] Sheikh-Bahaei, S; C.A. Hunt. 2011. "Enabling clearance predictions to emerge from in silico actions of quasi-autonomous hepatocyte components." *Drug Metab. Dispos*. 39(10):1910- 1920.

[11] Park, S.; S.H. Kim; G.E. Ropella; S.H. Kim; M.S. Roberts; C.A. Hunt. 2010. "Tracing multiscale mechanisms of drug disposition in normal and diseased livers." *J. Pharmacol. Exp. Ther*. 334(1):124-136.

[12] Ropella, G.E.; R.C. Kennedy; C.A. Hunt. 2012. "Falsifying an Enzyme Induction Mechanism within a Validated, Multiscale Liver Model." *Int. J. Agent Technol. Sys*. 4(3):1-14

[13] Kim, S.H.; S. Park; G.E. Ropella; C.A. Hunt. 2010. "Agent-directed tracing of multi-scale drug disposition events within normal and diseased In Silico Livers." *Int. J. Agent Technol. Systems* 2(3):1-19.

[14] Han, D.; R. Canali; D. Rettori; N. Kaplowitz. 2003. "Effect of glutathione depletion on sites and topology of superoxide and hydrogen peroxide production in mitochondria." *Mol Pharmacol*. Nov;64(5):1136-44.

[15] Win, S.; T.A. Than; J.C. Fernandez-Checa; N. Kaplowitz. 2014. "JNK interaction with Sab mediates ER stress induced inhibition of mitochondrial respiration and cell death." *Cell Death Dis*. Jan 9;5:e989.

[16] Ni, H.M.; J.A. Williams; H. Jaeschke; W.X. Ding. 2013. "Zonated induction of autophagy and mitochondrial spheroids limits acetaminophen-induced necrosis in the liver." *Redox Biol.* 1(1):427–432.

[17] Patel, S.J.; J.M. Milwid; K.R. King; S. Bohr; A. Iracheta-Velle; M. Li; A. Vitalo; B. Parekkadan; R. Jindal; M.L. Yarmush. 2012. "Gap junction inhibition prevents drug-induced liver toxicity and fulminant hepatic failure." *Nat Biotechnol*. Jan 15;30(2):179-83.

[18] Stutchfield, B.M.; S.J. Forbes. 2013. "Liver sinusoidal endothelial cells in disease--and for therapy?" *J Hepatol*. Jan;58(1):178-80.

Mod. 8(1), 35.